PHILOSOPHICAL TRANSACTIONS OF THE ROYAL SOCIETY A MATHEMATICAL, PHYSICAL & ENGINEERING SCIENCES

Ultrafast Optical Signal Processing Using Semiconductor Laser Amplifiers

R. Schnabel, R. Ludwig, W. Pieper, S. Diez and H. G. Weber

Phil. Trans. R. Soc. Lond. A 1996 **354**, 733-744
doi: 10.1098/rsta.1996.0027

Ultrafast optical signal processing using semiconductor laser amplifiers

By R. Schnabel, R. Ludwig, W. Pieper, S. Diez, H. G. Weber
Heinrich-Hertz-Institut für Nachrichtentechnik Berlin GmbH, Einsteinufer 37, 10587 Berlin, Germany

Optical fibres exhibit a bandwidth of about 50 THz, which enables data transmission in excess of 100 Gbit s^{-1}. This potential for ultrafast optical signal transmission stimulates the research on appropriate functional devices for optical switching and optical signal processing in general. A promising device is the semiconductor laser amplifier (SLA). It enables optical signal processing in the femtosecond range when it is operated under conditions where intraband dynamics with subpicosecond time constants are dominating. A suitable experimental technique for operating the SLA under these conditions is four-wave mixing.

Based on this technique, various applications for optical signal processing have been investigated, such as optical switches, demultiplexers, wavelength converters and phase conjugators. In this article we describe these experiments and discuss the advantages and disadvantages of optical signal processing using SLAs.

1. introduction

Fibre optic transmission is a well-established technique today. However, routing, switching and other signal-processing operations are still performed electrically by use of opto-electronic conversion. We expect many improvements in today's communication systems when no opto-electronic conversion is involved and when signal processing is performed on the signal while it is still in the form of light. For example, one expects a more efficient use of the transmission bandwidth of the optical fibre and perhaps also simple and less expensive devices for signal processing. Especially, devices in which light signals are controlled by light itself are very promising because data signals and control signals may be transmitted in the same optical fibre.

A device with a large potential for all-optical signal processing is the semiconductor laser amplifier (SLA). In addition to its ordinary application as a gain element, the SLA may play an important role as a functional device, such as an optical switching gate or frequency converter, etc. (see, for example, Weber *et al.* 1991). The main advantages of this device are optical gain, compactness and the potential for opto-electronic integration. However, the applications seem to be restricted to a time regime slower than about 100 ps, as determined by the free carrier lifetime. On the other hand, much faster effects (50–650 fs) based on intraband dynamics (carrier heating, spectral hole burning) in semiconductor devices are known (see, for example, Eisenstein *et al.* 1991). In the present paper, we focus our interest on the SLA as a functional device operating in the ultrafast time regime (time constant smaller than 1 ps), as determined by intraband dynamics.

Phil. Trans. R. Soc. Lond. A (1996) **354**, 733–744
Printed in Great Britain

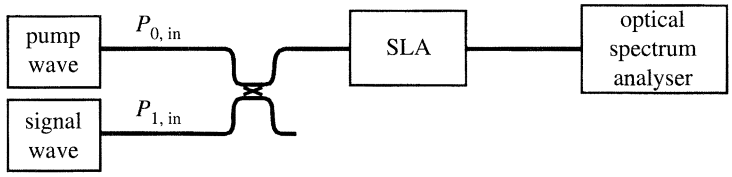

Figure 1. Set-up for FWM experiments with pump wave and signal wave.

In this article the following applications are considered: wavelength conversion of optical data signals; operation as a demultiplexer; and, finally, operation as an optical phase conjugator (OPC) for the compensation of deterministic pulse distortions caused by fibre dispersion and nonlinear self-phase modulation in the fibre. All experiments reported here have in common that they use four-wave mixing (FWM), based on the ultrafast gain dynamics in SLA, which promises processing of data rates in excess of 100 Gbit s^{-1}.

2. Four-wave mixing in a semiconductor laser amplifier

FWM in a SLA has been studied extensively in recent years. Examples of publications in 1994 include Uskov *et al.* (1994), Zhou *et al.* (1994), Kikuchi *et al.* (1994) and D'Ottavi *et al.* (1994). An arrangement often investigated in theory and experiment is as follows (see figures 1 and 2). Two optical fields, a pump wave (frequency f_0, output power P_0 at the SLA) and a signal wave (frequency f_1, output power P_1), both propagating in the same direction and with the same state of polarization, are coupled into a SLA. The superposition of both fields in the SLA leads to modulation of the gain medium at the beat frequency $\Delta f = f_0 - f_1$ (and multiples of Δf), which causes a dynamical index and gain grating. For small frequency spacing ($\Delta f < 10$ GHz), the physical mechanism behind FWM is predominantly carrier density modulation (interband dynamics). For large frequency spacing ($\Delta f > 10$ GHz), the efficiency of carrier density modulation decreases strongly and modulation of the carrier distribution (e.g. spectral hole burning and carrier heating) becomes important. Light scattering from the gain and refractive index grating generates two new light waves (output powers P_{-1} and P_2 in figure 2) which are frequency shifted from the two input waves by the beat frequency Δf. If the signal wave (P_1) is modulated, one of the newly generated waves (P_{-1}) represents a frequency-shifted and phase-conjugated replica of this data signal. The frequency conversion range may extend over the entire gain spectrum of the SLA. The maximum frequency shift obtained in our experiments was $2\Delta f = 15$ THz (corresponding to 120 nm).

Figure 3 depicts the output powers P_{-1}, P_0, P_1, P_2 and the ASE-powers (amplified spontaneous emission power) at the wavelengths (λ_{-1} and λ_2) corresponding to the P_{-1} and P_2 signals versus the input power $P_{1,\mathrm{in}}$. In this experiment, both input waves were continuous waves with the same input powers. The resolution of the optical spectrum analyser was 0.1 nm. Also indicated in this figure is the FWM-efficiency, i.e. the ratio $P_{-1}/P_{1,\mathrm{in}}$ and the signal-to-background ratio SBR $= P_{-1}/\mathrm{ASE}(\lambda_{-1})$. It is evident from the results in figure 3 that the FWM-efficiency has a maximum between -15 and -10 dBm input power and decreases for higher input powers. On the other hand, the SBR ratio reveals a steady increase with increasing input power. Several groups performed studies on the FWM-efficiency (see, for example, Tiemeijer 1991) and the SBR ratio (see, for example, Tatham *et al.* 1993*b*). In a system application,

PHILOSOPHICAL TRANSACTIONS OF THE ROYAL SOCIETY A MATHEMATICAL, PHYSICAL & ENGINEERING SCIENCES

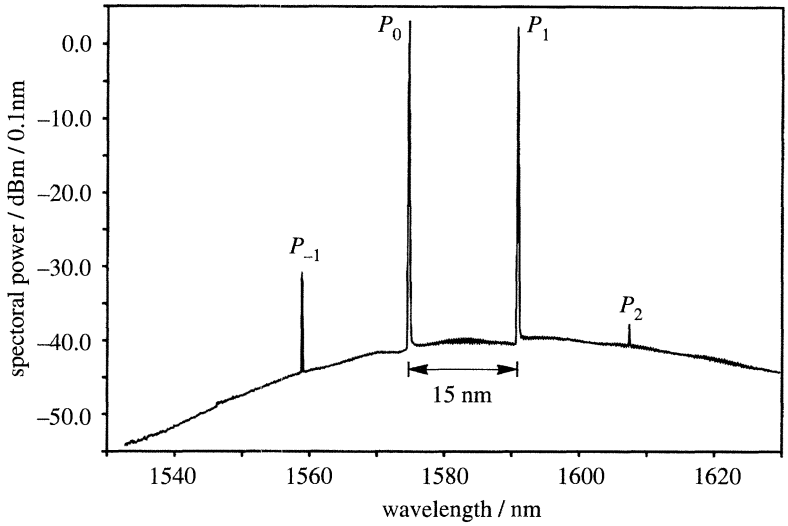

Figure 2. FWM spectrum taken at the output of the SLA.

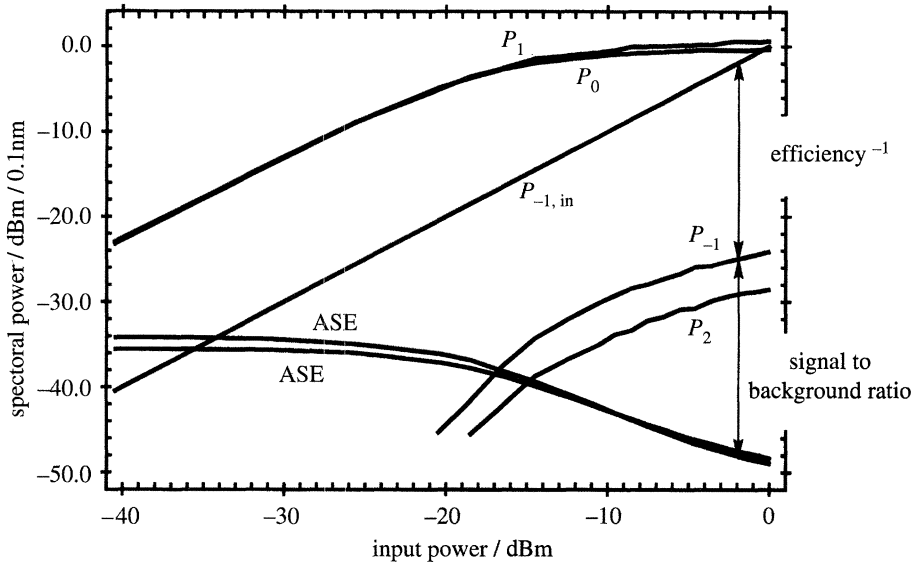

Figure 3. Dependence of the spectral power in the FWM spectrum (figure 2) on the input power.

the optical SBR is related to the electrical signal-to-noise ratio, which determines the quality of the transmission system.

3. Wavelength conversion

The simple FWM scheme described in § 2 may be used for wavelength conversion of optical data signals. Because of the fast time constants of intraband dynamics, both the data rate and the conversion span are essentially limited only by the gain bandwidth (≈ 20 THz) of the SLA. Using this scheme, several experiments were reported: 25 nm wavelength conversion of a train of 30 ps pulses with a repetition rate of 3 GHz (Schnabel *et al.* 1993); 20 nm wavelength conversion of a 622 Mbit s^{-1} data

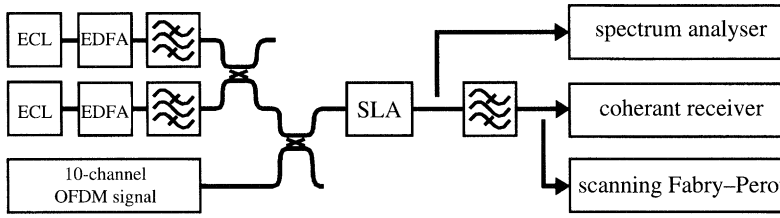

Figure 4. Experimental arrangement for the frequency conversion of a 10-channel OFDM signal: ECL, external cavity laser; EDFA, erbium-doped fibre amplifier; OFDM, optical frequency division multiplexing.

signal (Tatham *et al.* 1993*b*); 15 nm wavelength conversion of a 18 Gbit s^{-1} data signal (Schnabel *et al.* 1993). However, one drawback prohibits the direct employment of this scheme to practical wavelength converters. The state of polarization of the incoming data signal has to be constant. Therefore, a polarization-independent scheme was developed using two pump waves with identical polarization. The interference of these pump waves results in a modulation of the gain medium, as described in § 2. An additional signal wave with an arbitrary state of polarization is affected by this modulation. A conversion experiment was realized with a 10-channel optical frequency division multiplexed (OFDM) TV-distribution system (Schnabel *et al.* 1994).

Figure 4 depicts the experimental setup and figure 5 depicts the optical spectrum at the output of the SLA. In the experiment, we used a strained layer MQW semiconductor laser amplifier as a frequency converter. The SLA is described in detail in Magari *et al.* (1991). Two continuous pump waves with a frequency spacing of $\Delta f = 275$ GHz (wavelength 1563.3 nm and 1565.6 nm, 0.5 dBm and 4.1 dBm, respectively, at the input of the SLA) and 10 FSK-signals of a coherent 10-channel TV-distribution system (Hilbk *et al.* 1992) were fed into the SLA. The frequency spacing Δf was equal to the desired frequency conversion range. The two pump waves caused FWM in the SLA. As a result, the output spectrum of the SLA showed not only the typical FWM-spectrum around the two pump waves, but also that each channel (carrier frequency f) of the 10-channel system had sidebands at the frequencies $f \pm \Delta f$. We obtained two frequency-shifted replicas (multichannel sidebands) of the input data signals additionally to the amplified original signals, as shown in figure 5.

We also measured the spectrum by a scanning Fabry–Perot (figure 6) to get a higher resolution of the converted signal. For this measurement, the original spectrum of the OFDM signal was attenuated by an optical filter and the conversion range was changed to 180 GHz. The high resolution of this measurement enables us to see the peaks of the wide band FSK modulation on each modulated channel. In addition, we proved that the succession of the channels in the spectrum is not changed by the conversion scheme. The unmodulated carrier wave (C in figure 6) lies on the left-hand side in the spectrum of the original as well as in the frequency-shifted replica.

To investigate the polarization sensitivity and the cross-talk of the converted data signals, we performed BER measurements. In these experiments, an optical filter with a bandwidth of about 1 nm was used to suppress the pump waves and the original signal. Figure 7 shows BER measurements for the conversion of 1 (dots) or 10-channels (triangles) as a function of the received signal power at the input of the optical front-end of a polarization diversity receiver. The slight bending of the BER curve is due to the fixed threshold of the decision circuit in the receiver, which can also be seen in back-to-back BER measurements. The sensitivity degradation,

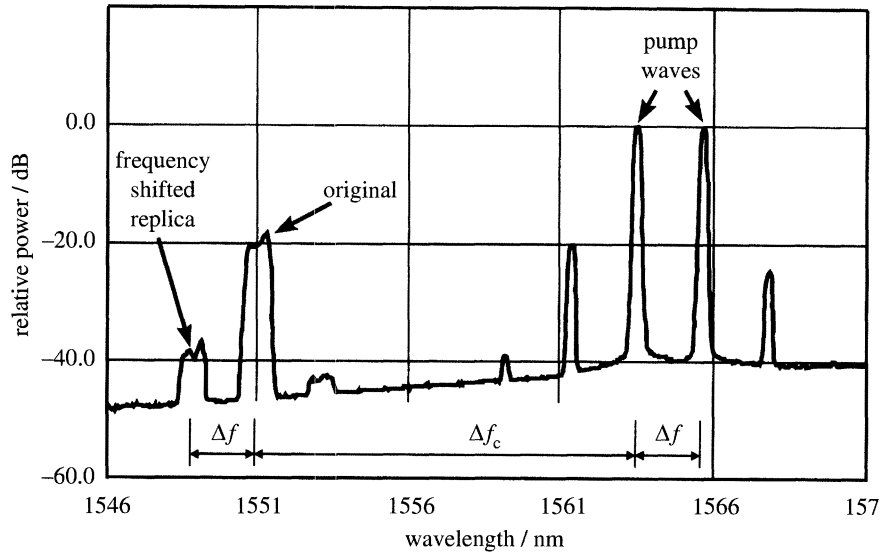

Figure 5. Optical spectrum at the output of the SLA.

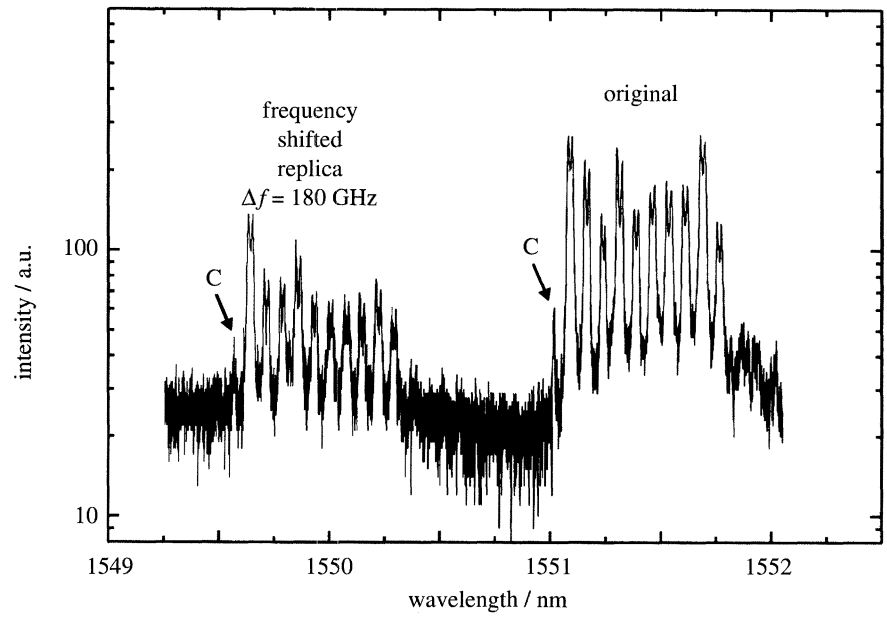

Figure 6. Optical spectrum taken with a scanning Fabry–Perot, showing the original OFDM signal and one of the frequency-shifted replica. C denotes the unmodulated carrier wave.

due to the transmission of 10-channels, amounts to 1 dB. To check the polarization dependence of the frequency conversion, the state of polarization of the OFDM input signal was changed during BER measurements. A BER change corresponding to a sensitivity degradation of 1.5 dB was observed. To investigate the performance during transmission of real data, a 140 Mbit s^{-1} CMI coded TV signal was converted and received. No subjective transmission errors could be observed.

The experiment reported here shows a polarization-independent wavelength con-

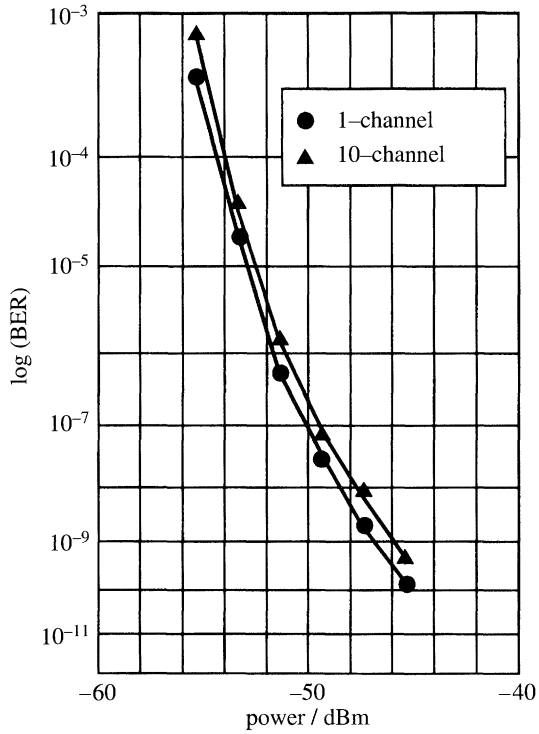

Figure 7. BER versus optical power at the frontend for 1-channel and 10-channel conversion.

version using FWM in a SLA. The conversion range of 275 GHz (≈ 2 nm) was determined only by constraints of the transmission system. The conversion efficiency of the SLA and the resulting SBR promise an increased conversion range. Furthermore, instead of a 10-channel OFDM signal with an overall bandwidth of 90 GHz, it seems to be straightforward to achieve wavelength conversion of an OTDM signal with a data rate having a comparable broad spectrum.

4. Demultiplexer and AND gate

In the setup in figure 1 with the corresponding spectrum in figure 2, we assume in the following that both input signals are pulse trains. The newly generated signals (output powers P_{-1} and P_2) occur only if pulses from both trains are simultaneously copropagating in the SLA. Therefore, this scheme can be used as an optical AND gate (Schnabel *et al.* 1993). The application of such an AND gate as an optical demultiplexer was investigated in the following experiment (Ludwig & Raybon 1993).

A simplified schematic of the experimental setup is shown in figure 8. The pulses of a 1546.5 nm tuneable external cavity laser ($\mathrm{MLL_s}$), mode-locked at 5 GHz, were modulated by a 2^7-1 pseudorandom bit stream of a BER transmitter. The 5 Gbit $\mathrm{s^{-1}}$ signal was passively multiplexed to 20 or 40 Gbit $\mathrm{s^{-1}}$. The pulse width of the source was 12 ps. To avoid coherent superposition at 40 Gbit $\mathrm{s^{-1}}$, the last stage of the multiplexer did polarization multiplexing. The signal was transmitted over 25 km of dispersion-shifted fibre to the demultiplexer, where pulses from a second mode-locked external cavity laser ($\mathrm{MLL_p}$) were added to the signal via a 3 dB coupler with the same state of polarization. Simple adjustment of the pump polarization enabled us to

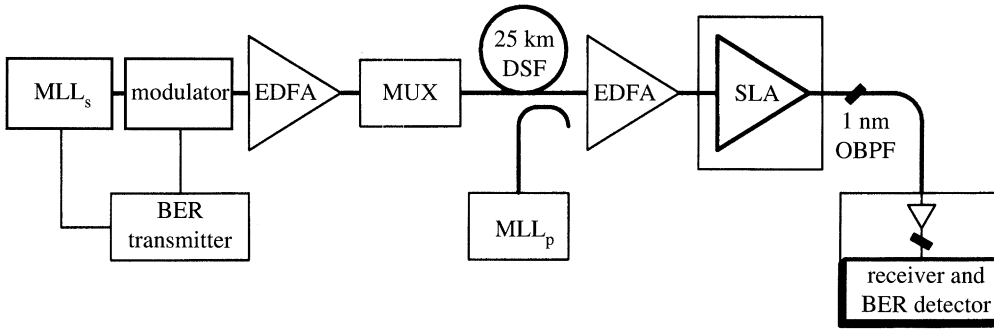

Figure 8. Experimental setup for demultiplexing.

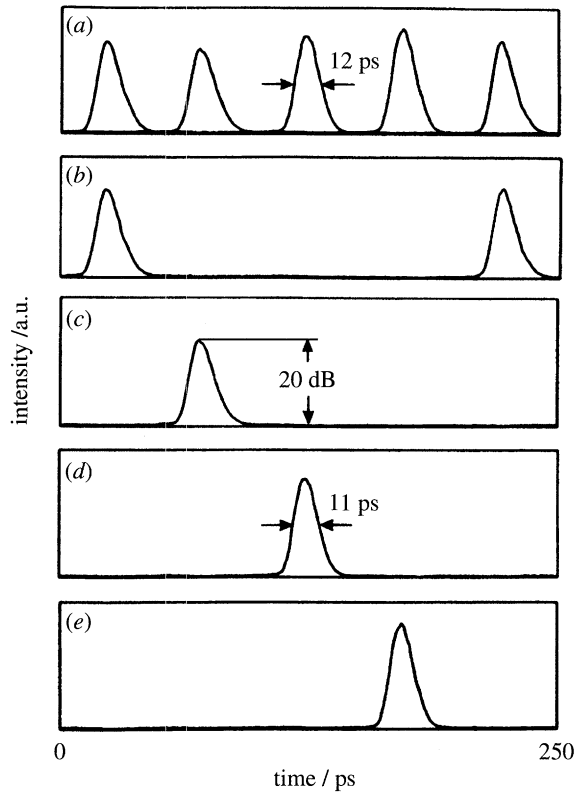

Figure 9. Streak camera measurement of multiplexed 20 GHz pulse train (*a*), and four demultiplexed 5 GHz pulse trains (*b*)–(*e*).

select each 20 Gbit s^{-1} bit stream. The erbium-doped fibre amplifier (EDFA) boosted the optical input power of the pump ($P_p = 150\ \mu W$) and the signal ($P_s = 31\ \mu W$) by 20 dB. The output of the EDFA was fed to a packaged polarization-insensitive bulk SLA (Lin *et al.* 1990). The SLA was biased at 200 mA and measured to be saturated by 20 dB by the input signals. The frequency converted signal at $\lambda = 1539.5$ nm was selected out of the output spectrum with a 1 nm optical bandpass interference filter (OBPF). The received signal was optically preamplified by 30 dB in an EDFA, filtered by a 0.7 nm interference filter. Then it was sent to a streak camera for accurate pulse measurement (not shown in the figure) or it was fed to the BER receiver.

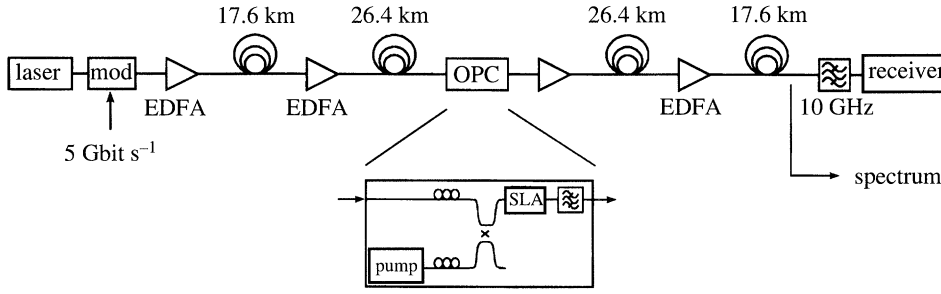

Figure 10. Experimental set-up with SLA as OPC.

Figure 9 depicts streak camera recordings of a multiplexed 20 GHz pulse train (figure 9*a*) and individual demultiplexed 5 GHz pulse trains (figures 9*b*, *c*, *d*, *e*). No measurable energy from the other channels was observed in the demultiplexed signal and an on–off ratio of 20 dB was obtained. BER measurements after transmission over a short length of fibre were performed. Compared to the baseline sensitivity of −36 dBm, a 2 dB penalty and a slight slope difference were obtained for all four demultiplexed channels. The BER performance for each channel was essentially the same and there was no indication of an error floor down to BER $= 10^{-11}$. The 2 dB system penalty can be attributed to intersymbol interference due to the low-frequency carrier density dynamics in the SLA.

Although the results of the described experiments are very promising, it should be mentioned that a realistic demultiplexer has to be polarization independent. Furthermore, the problem of synchronization of the incoming data signal with the sampling pulse train was not considered. However, an all-optical demultiplexer based only on semiconductor devices has the potential for monolithic integration on InP to form a complete demultiplexer–receiver for all channels on one chip.

5. Optical phase conjugation

A characteristic for the FWM-scheme, as described in § 2, is the appearance of new wavelength components (powers P_{-1} and P_2 in figure 2). If P_1 represents a data signal described by the optical field E, then P_{-1} represents a replica of this data signal and may be described by an optical field which is proportional to E^*, which is the phase-conjugate optical field to E. Optical phase conjugation (OPC) was used to compensate for pulse distortions due to fibre dispersion or fibre nonlinearity. The attractiveness of this application arises from the demands of long-haul transmission on standard fibres, where the capacity is limited by the interaction of chromatic dispersion and nonlinear self-phase modulation. While the compensation of fibre dispersion was shown by Tatham *et al.* (1993*a*), this paper focuses on the results of an experiment concerning the compensation of fibre nonlinearity (Pieper *et al.* 1994). It should be mentioned that the FWM-scheme used for this experiment is polarization dependent. A polarization-independent scheme for OPC was proposed by (Jopson & Tench 1993).

The experimental setup is depicted in figure 10. The total system length was ∼ 90 km of standard single-mode fibre (dispersion 17 ps km^{-1} nm^{-1}). At the transmitter, a $2^7 - 1$ PRBS signal with a bit rate of 5 Gbit s^{-1} was generated by external modulation. The input signal was set to 1566 nm with a power of −3.6 dBm at the input of the SLA in the OPC. The pump wavelength was 1563 nm (8.1 dBm input

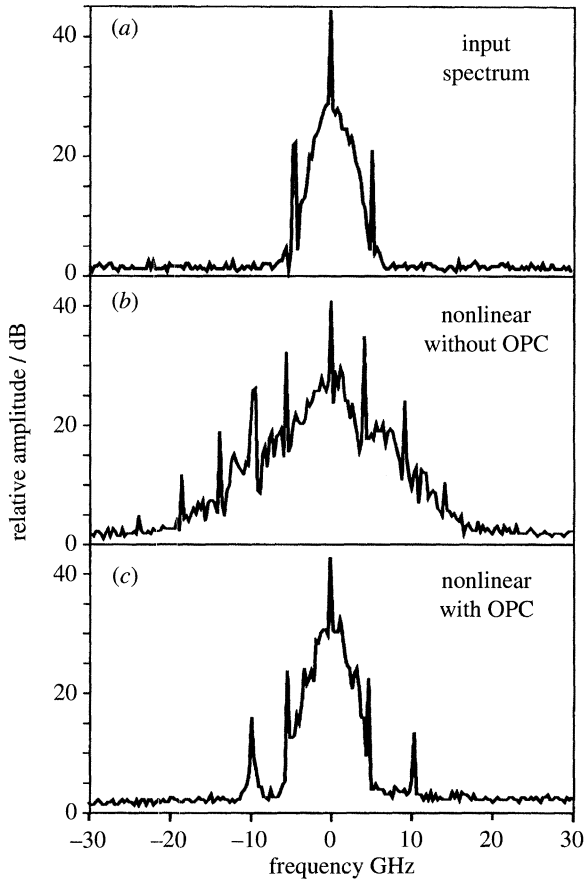

Figure 11. Experimental spectra ($P_0 = 13$ dBm) taken behind the modulator (a) and before the 10 GHz filter in figure 10 without OPC (b) and with OPC (c).

power). The newly generated output signal at 1560 nm was selected by optical band-pass filters. The SLA (Magari *et al.* 1991) was driven at 300 mA and 20 °C. Several EDFA were used in the transmission span.

To quantify the input power limitations for each fibre segment imposed by stimulated-Brillouin scattering (SBS) we carried out CW measurements. We conclude that the impact of SBS on the spectrum of the modulated signal becomes noticeable for average input power levels of ~ 12 dBm, reaching a Brillouin threshold at ~ 13 dBm. As a rough estimation we can classify a specific system configuration as quasi-lossless and, therefore, symmetrical if the nonlinear phase shift ϕ_{nl} between two consecutive amplifiers satisfies the inequality $\phi_{\mathrm{nl}} = \gamma P_0 L_{\mathrm{eff}} < 1$. Here γ is the nonlinearity coefficient, P_0 the peak power and L_{eff} the effective length. The latter is given by $L_{\mathrm{eff}} = [1 - \exp(-\alpha\Delta_{\mathrm{OA}})]/\alpha$, with the fibre attenuation coefficient α and Δ_{OA} the amplifier spacing. As a peak power of 13 dBm for each fibre segment (as discussed above) results in a nonlinear phase shift of $\phi_{\mathrm{nl}} = 0.7$, the described setup was considered suitable for generating sufficient SPM-induced spectral broadening as well as for studying the impact of OPC on SBS. The optical power distribution was chosen to be approximately identical in both spans.

First we studied the impact of OPC on the nonlinearity-induced spectral deformations with a heterodyne spectrometer. The results in figure 11 clearly illustrate that

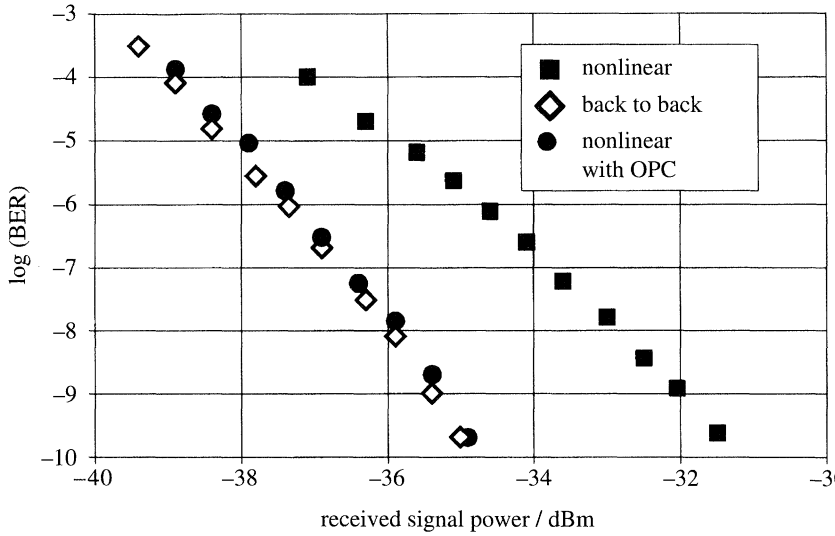

Figure 12. BER measurement for OPC experiment ($P_0 = 13$ dBm).

the significant spectral broadening caused by SPM can be compensated for with high efficiency. In contrast, the two discrete spectral lines in figure 11 reveal that the SBS initiated by ASE could not be compensated for by OPC. To evaluate the nonlinear performance of the optically filtered system with and without OPC, we determined the power penalty from a study of the bit error rate curves. As can be seen from figure 12, penalties of several dB are induced when no OPC is used. These penalties disappear by low optical power ($P_0 \approx 4$ dBm) measurements. This confirms that fibre dispersion is not the cause of these penalties. With OPC, however, nearly penalty-free system performance was achieved for average input power levels up to $P_0 = 13$ dBm, proving that the system is essentially insensitive to fibre nonlinearity. To confirm the experimental results, calculations were performed simulating the setup shown in figure 10 by numerically solving the nonlinear Schrödinger equation. The calculated spectra exhibit good agreement with experimental results (Pieper *et al.* 1994).

The experiment showed good agreement with the theoretical calculations that FWM in a SLA is an attractive technique to compensate for pulse distortions due to self-phase modulation.

6. Discussion

In this article we reported on optical signal processing based on the optical nonlinearity associated with intraband dynamics in SLAs. Examples reported included wavelength conversion, fast optical switching for demultiplexing of optical data signals and compensation of pulse distortion due to fibre dispersion and fibre nonlinearity. The processing speed can be faster than 1 ps and, therefore, enables processing of data signals with bit rates in excess of 100 Gbit s^{-1}. Fast optical signal processing is also possible using the optical nonlinearity of the fibre. However, signal processing using fibre nonlinearity needs long fibre lengths or large optical power. For instance, optical pulses of about 1 W peak power in 1 km of optical fibre length are required to realize an optically controlled switch based on the nonlinear optical loop mirror (Patrick *et al.* 1993). The advantages of the SLA are: the compactness of the device;

PHILOSOPHICAL TRANSACTIONS OF THE ROYAL SOCIETY A MATHEMATICAL, PHYSICAL & ENGINEERING SCIENCES

the low energy consumption; the operation at a low signal level of about 1 mW; the combination of functionality with gain; and finally the possible integration with other InP devices. Disadvantages of the semiconductor laser amplifier as functional device are: spontaneous emission noise, which is added to the signal, and coupling losses.

We restricted our discussion on applications using the fast intraband dynamics in the semiconductor laser amplifier. Interband dynamics (change of carrier density) enables an even richer variety of optical signal processing applications. As well as the nonlinear optical mode of operation it additionally allows the opto-electronic mode of operation. The large spectrum of applications based on inter- and intraband dynamics shows that the SLA has the potential to be a very general device for optical signal processing.

The work was supported by the Bundesminister für Bilding, Wissensdaft, Forschung und Technologie of the Federal Republic of Germany in the national Photonic Research Program.

References

D'Ottavi, A., Iannone, E., Mecozzi, A. *et al.* 1994 Investigation of carrier heating and spectral hole burning in semiconductor amplifiers by highly nondegenerate four-wave mixing. *Appl. Phys. Lett.* **64**, 2492–2494.

Eisenstein, G., Wiesenfeld, J., Wegener, M. *et al.* 1991 Ultrafast gain dynamics in 1.5 μm multiple quantum well optical amplifiers. *Appl. Phys. Lett.* **58**, 158–160.

Hilbk, U., Burmeister, M., Hermes, T. & Hoen, B. 1992 Absolute stabilized 10 channel TV-distribution system with microprocessor controlled subscriber station. Technical Digest, EFOC LAN Paris, pp. 144–146.

Jopson, R. & Tench, R. 1993 Polarisation-independent phase conjugation of lightwave signals. *Electron. Lett.* **29**, 2216–2217.

Kikuchi, K., Amano, M., Zah, C. & Lee, T. 1994 Analysis of origin of nonlinear gain in 1.5 μm semiconductor active layers by highly nondegenerate four-wave mixing. *Appl. Phys. Lett.* **64**, 548–550.

Ludwig, R. & Raybon, G. 1993 All-optical demultiplexing using ultrfast four-wave mixing in a semiconductor laser amplifier at 20 Gbit s^{-1}. Technical Digest, ECOC Montreux, pp. 57–59.

Lin, M., Piccirilli, A., Twu, Y. & Dutta, N. 1990 Temperature dependence of polarization characteristics in buried facet demiconductor laser amplifiers. *IEEE J. Quantum. Electron.* **26**, 1772–1778.

Magari, K., Okamoto, M. & Noguchi, Y. 1991 1.55 μm polarization-insensitive high-gain tebsile-strained-barrier MQW optical amplifier. *IEEE Photon. Technol. Lett.* **3**, 998–1000.

Patrick, D., Ellis, A. & Spirit, D. 1993 Bit-rate flexible all-optical demultiplexing using a nonlinear loop mirror. *Electron. Lett.* **29**, 702–703.

Pieper, W., Kurtzke, C., Schnabel, R. *et al.* 1994 Nonlinearity-insensitive standard-fibre transmission based on optical-phase conjugation in a semiconductor laser amplifer. *Electron. Lett.* **30**, 724–726.

Schnabel, R., Hilbk, U., Hermes, T. *et al.* 1994 Polarization insensitive frequency conversion of a 10-channel OFDM signal using four-wave mixing in a semiconductor laser amplifier. *IEEE Photon. Technol. Lett.* **6**, 56–58.

Schnabel, R., Pieper, W., Ehrhardt, A., Eiselt, M. & Weber, H. G. 1993 Wavelength conversion and switching of high speed data signals using semiconductor laser amplifiers. *Electron. Lett.* **29**, 2047–2048.

Schnabel, R., Pieper, W., Ludwig, R. & Weber, H. G. 1993 Multiterahertz frequency conversion of a picosecond pulse train using nonlinear gain dynamics in a 1.5 μm MQW semiconductor laser amplifier. *Electron. Lett.* **29**, 821–822.

PHILOSOPHICAL TRANSACTIONS OF THE ROYAL SOCIETY A MATHEMATICAL, PHYSICAL & ENGINEERING SCIENCES

Tatham, M., Sherlock, G. & Westbrook, L. 1993*a* Compensation of fibre chromatic dispersion by mid-way spectral inversion in a semiconductor laser amplifier. Technical Digest, ECOC Montreux, pp. 61–64.

Tatham, M., Sherlock, G. & Westbrook, L. 1993*b* 20 nm optical wavelength conversion using nondegenerate four-wave mixing. *IEEE Photon. Technol. Lett.* **5**, 1303–1306.

Tiemeijer, L. 1991 Effects of nonlinear gain on four-wave mixing and asymmetric gain saturation in a semiconductor laser amplifier. *Appl. Phys. Lett.* **59**, 499–501.

Uskov, A., Mørk, J. & Mark, J. 1994 Wave mixing in semiconductor laser amplifiers due to carrier heating and spectral hole burning. *IEEE J. Quantum. Electron.* **30**, 1769–1781.

Weber, H. G., Großkopf, G., Ludwig, R., Patzak, E. & Schnabel, R. 1991 Optical signal processing using semiconductor laser amplifiers. Technical Digest, ECOC/IOOC Paris, MoC2.1.

Zhou, J., Park, N., Dawson, J., Vahala, K., Newkirk, M. & Miller, B. 1994 Efficiency of broadband four-wave mixing wavelength conversion using semiconductor traveling-wave amplifiers. *IEEE Photon. Technol. Lett.* **6**, 50–52.

PHILOSOPHICAL TRANSACTIONS OF THE ROYAL SOCIETY A MATHEMATICAL, PHYSICAL & ENGINEERING SCIENCES